Investigation of microstructure evolution during AA6082 chips recycling through friction consolidation

Usman Aziz[1,a*], Uceu F.H. Suhuddin[2,b], Lars Rath[2,c], Léon F. Schröder[3,d], Volker Schmidt[3,e], Benjamin Klusemann[1,2,f]

[1]Institute for Production Technology and Systems, Leuphana University Lüneburg, Universitätsallee 1, Lüneburg, 21335, Germany

[2]Solid State Materials Processing, Institute of Material and Process Design, Helmholtz-Zentrum Hereon, Max–Planck-Straße 1, Geesthacht, 21502, Germany

[3] Institute of Stochastics, Ulm University, 89069 Ulm, Germany

[a]usman.aziz@leuphana.de, [b]uceu.suhuddin@hereon.de, [c]lars.rath@hereon.de, [d]leon.schroeder@uni-ulm.de, [e]volker.schmidt@uni-ulm.de, [f]benjamin.klusemann@leuphana.de

Key Words: Friction Extrusion, Friction Consolidation, Recycling, AA6082, Bonding and Microstructure

Abstract

Recycling aluminum chips remains a major challenge in aluminum manufacturing because it is difficult to retain the original quality alloy properties while reducing the carbon footprint and ensuring a sustainable process. This work investigates the microstructural evolution and bonding quality of compacted AA6082 chips processed through friction extrusion/consolidation. The residual material left inside the extrusion container after processing at a high extrusion ratio was analyzed using SEM, EDS, and EBSD to understand bonding mechanisms and microstructure evolution in front of the die. The SEM results show that voids are still present between the chips in the initial compacted material which already shows bonding, while these voids are reducing towards the die interface, particularly related to the present severe plastic deformation. EDS analysis confirms the presence of Al(Fe,Mn)Si intermetallic particles, which break and disperse in the matrix because of shear deformation due to die rotation. EBSD analysis reveals that grains are coarser near the base material, and subdivisions of grains near the die interface are significant because of continuous dynamic recrystallization.

1. Introduction

In general, recycling of aluminum (Al) chips can be done in two main ways: conventional recycling and direct conversion. In the conventional route, the chips are melted, cast into billets, and then processed further, for example by hot extrusion, to produce rods, wires, or similar products [1]. In contrast, direct conversion avoids melting and instead consolidates the chips into a solid part through solid-state methods. Additionally, direct conversion methods offer significant advantages over traditional remelting-based recycling. Remelting often leads to problems such as oxidation, buildup of impurities, and a loss of material due to the formation of brittle intermetallic phases [1]. These limitations become more severe for machining chips, whose irregular geometries and high specific surface areas promote rapid native oxide formation, thereby diminishing remelting efficiency [1, 2].

To address these limitations associated with machining chips, solid-state recycling approaches such as friction extrusion/consolidation (FE/FC) avoid melting and instead rely on frictional heating and severe plastic deformation (SPD), enabling microstructural refinement while minimizing oxidation

and energy consumption [3-5]. Recent studies have shown that FE can successfully produce functional aluminum products with reduced environmental impact, supporting its integration into sustainable manufacturing pathways. Furthermore, FE has been extensively applied to recycle Al alloy scrap through solid-state consolidation into extruded products such as wires, wide components (sheets) [6] and rods with improved mechanical properties thoroughly reported [4, 7-9].

Regarding Al scrap consolidation and bonding behavior investigations, Baffari et al. [5] reported that sheet-metal scrap processed by FC resulted in a compacted billet exhibiting variations in bonding quality along the billet height. Whereas material near the die interface (top region) was severely deformed and fully consolidated, showing complete bonding due to intense stirring and recrystallization, the intermediate region exhibited partial consolidation through solid-state welding between the chips. The bottom region was mainly compacted with limited metallurgical bonding and reduced mechanical integrity [5]. Additionally, Tang and Reynolds [10] obtained dense, well-bonded disks via FC of Al chips. The strongest bonding occurred in the recrystallized core region, while a recurring weakly bonded ring appeared near the bottom outer edge where deformation and heating were insufficient [10]. Similarly, Poy Ignacio et al. [11] demonstrated that FE at high extrusion ratio enables effective solid-state consolidation of Al chips, producing wires with good metallurgical bonding; however, excessive temperature buildup during processing promotes defect formation such as voids and cracks, which degrade mechanical properties along the wire length. On the other side, Mejbel et al. [12] investigated the consolidation of Al chips using FC with particular emphasis on chip-to-chip bonding mechanisms. The results revealed spatial variations in consolidation and bonding quality across the billet cross-section, governed by differences in heat generation, process parameters, plastic deformation, and material flow. Puleo et al. [13] analyzed variations in consolidation and bonding quality by studying the formation of chips-chips bonds during the friction-based solid-state process. It was found that conventional bonding criteria from processes like sintering or SPD were not suitable for chips bonding, so a new friction-specific bonding criterion was developed based on experiments and simulations. This model enabled prediction of bonding occurrence throughout the billet, addressing issues of incomplete consolidation in regions distant from the tool interface. The developed criterion accurately predicts consolidation and bonding success from parameters such as tool rotation speed, applied force, and consolidation time, making FC process design more reliable. In this regard, multi-step FC strategies were introduced, where multiple passes of stirring and consolidation improved bonding uniformity and microstructural integrity [14].

Although the consolidation and bonding behavior of aluminum chips have been extensively studied in the production of consolidated billets, comparatively little attention has been paid to the bonding characteristics of the residual material remaining inside the die during the FE process at high extrusion ratios. In particular, the evolution of chip–chip interfaces and their influence on consolidation during FE remain insufficiently understood. Despite the growing interest in FE, the microstructural development from the base material region, i.e. compacted chips, towards the die interface, which in the end determined the final properties of the extrudate, has not been systematically investigated. Therefore, a detailed examination of this residual consolidated zone is essential to clarify the underlying deformation and bonding mechanisms. Accordingly, this study systematically examines the residual AA6082 material from chips at multiple locations in front of the die to elucidate their bonding behavior and microstructural evolution.

2. Materials and Methodology

The FE machine FE 100 (BOND Technologies), shown in Fig. 1, was employed. A total of 300 g of AA6082-T6 alloy chips were processed. The chips were produced during a turning operation on a lathe machine on clean AA6082 rod material, without the application of coolant or lubricant. The chips were initially compacted inside the extrusion container through several compression steps performed without rotation. This procedure resulted in approximately 62% compaction, corresponding to a bulk density of about 1.67 g/cm.

Figure 1. Illustration of Friction Extrusion Machine FE100 (Bond Technologies) and process principles [15].

The friction extrusion process was operated at a target force of 400 kN, with a spindle speed of 300 RPM. A featureless die with a planar face and a two-step inflow angle of 7.5˚ and 15˚, leading to a 1.5 mm die bore or extrusion ratio (ER) of 1111, was used. Within this study, the focus is on the residual material, i.e. the material in front of the die. Therefore, due to the high extrusion ratio, this process can also be considered as friction consolidation for the residual material. The residual material was cut, ground, and polished in colloidal silica according to standard metallographic procedures. The prepared sample was analyzed at 20 kV through an FEI Quanta 650 field emission gun (FEG) scanning electron microscope (SEM) equipped with a TSL OIM electron backscatter diffraction (EBSD) system at step size of 0.2 µm and an EDAX energy dispersive X-ray spectroscopy (EDS) system.

3. Results and Discussions

a. SEM Analysis

The macrograph from the base material to the die interface is presented in Fig. 2, highlighting also the specific locations where microstructural analysis was conducted. The evolution of the macrostructure is divided into three distinct zones. The first one is feedstock/compaction zone, where the alignment of chips changes during compaction and the feedstock material becomes vertically aligned due to compressive forces; in this zone, chip boundaries remain clearly visible, indicating the absence of metallurgical bonding. The second zone is thermo-mechanically affected zone (TMAZ) 2, an intermediate zone in which the chips are drawn in the direction of material flow towards the die–feedstock interface, and the chip boundaries gradually fade, suggesting the initiation of diffusion and partial metallurgical bonding. The third zone is TMAZ 1, the zone closest to the die interface, where chip boundaries completely disappear, and a fine-grained microstructure

is formed because of severe plastic deformation, indicating full metallurgical bonding. The material from TMAZ 1 serves as primary source of the extruded material, where the extruded wire is not focused on this study.

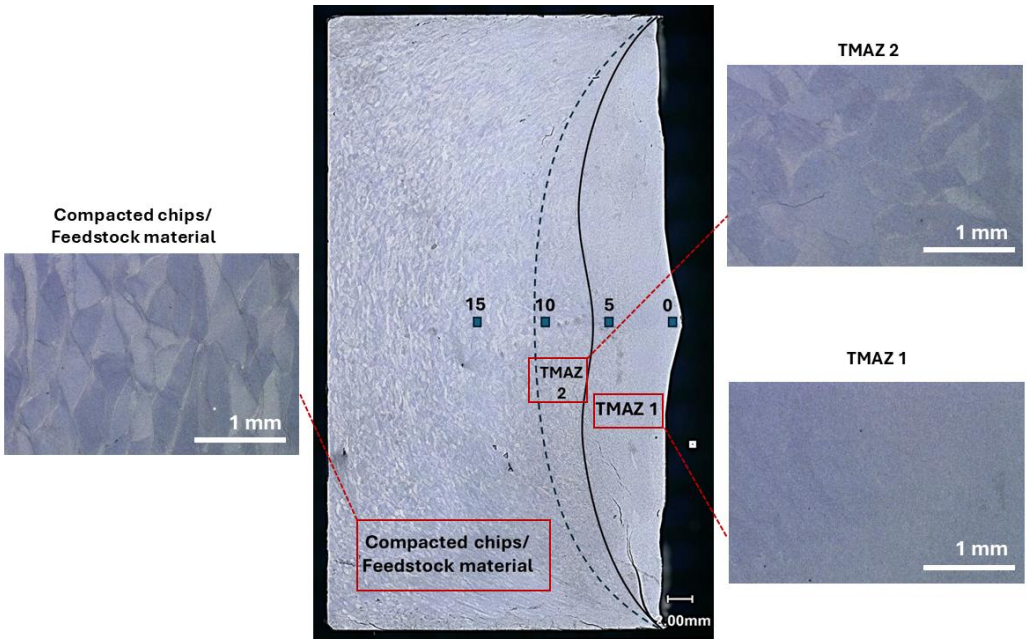

Figure 2. Macrograph of the residual material after friction extrusion of Al chips at distances of 15, 10, 5, and 0 mm from the die–material interface, where 15 mm corresponds to the compacted chip region and 0 mm is adjacent to the die interface.

In Fig. 3, SEM micrographs obtained at distances of 15, 10, 5, and 0 mm from the die-feedstock interface are presented. The micrographs reveal distinct microstructural variations across the residual material, where the region at 15 mm is representative for the compacted chips, while the 0 mm position is adjacent to the die, representative of the extruded material.

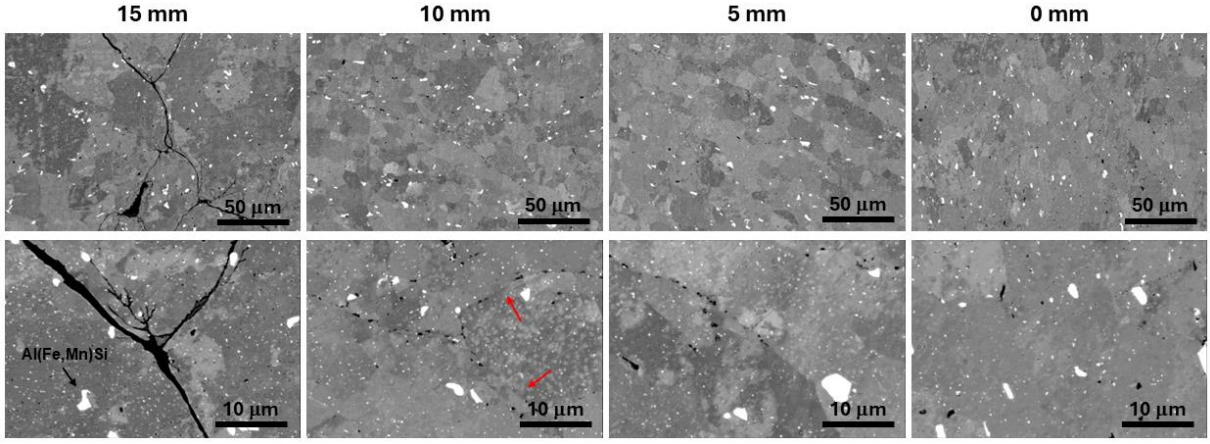

Figure 3. Micrographs taken from the base material interface towards die-feedstock interface at 15 mm, 10 mm, 5 mm, and 0 mm, see Fig. 2.

Chemical composition analysis by EDS reveals that the bright particles in the microstructures are Al(Fe,Mn)Si intermetallic particles, which were originally formed during the alloy's casting/solidification. Fe and Mn have low solubility in Al, therefore, excess Fe and Mn segregate, forming the Al(Fe,Mn)Si intermetallic. During FE/FC, the particles do not dissolve, instead the particles are getting smaller and dispersed in the Al matrix towards the die-feedstock interface. Shear deformation induced by the tool rotation broke the large particles into smaller sizes and distributed them randomly in the Al matrix [16].

The bonding behaviour between base material and die interface can be summarized as follows: At 15 mm (compacted chips region), there are voids between the chips indicating very less deformation by the die. At 10 mm, most of the voids between the chips are closed, but smaller discontinuous voids still exist, indicating compressive deformation from the die. Additionally, there are indications of significant metallurgical bonding between the chips (highlighted by red arrows in Fig. 3) pointing out that the process temperature and compressive force are getting high enough to induce metallurgical bonding. This progression in metallurgical bonding indicates that bonding quality increases steadily due to compression induced by the die's axial force, followed by shearing promoted by die rotation and a rise in temperature as the material approaches the die interface. The transformation of the chips boundary from feedstock material to the 10 mm area suggests that a sintering-like process occurred during FE/FC, leading to voids as voids are initially larger at the early stage; however, during sintering they tend to shrink to a minimum size. In some regions the voids may disappear completely, while in others they remain [17]. Heat and deformation bring chip surfaces into intimate contact, initiating diffusion and plastic flow. These mechanisms cause neck formation at particle contacts, followed by neck growth through surface and lattice diffusion, leading to particle coalescence and densification. However, these mechanisms progress unevenly; some regions even fail to fully bond, leaving voids. Moving further, at 5 mm, metallurgical bonding improves, and the extent of bonding gaps decreases, with the remaining unbonded zones forming a wavy and discontinued path indicating shear deformation, i.e., induced by die rotation. At the die interface, there are no visible voids or chips boundaries anymore; therefore, the material is characterized as consolidated. The seen pores in the micrographs, randomly distributed, are most likely formed during metallographic sample preparation due to particle drop-off.

b. EBSD Analysis

The microstructures obtained at distances of 15, 10, 5, and 0 mm are shown in Fig. 4. In the inverse pole figure maps (upper maps), grain boundaries are categorized according to the misorientation angle between adjacent grains, where misorientation angles between 2˚ and 15˚ are classified as low-angle grain boundaries (LAGBs) and misorientation angles greater than 15˚ are defined as high-angle grain boundaries (HAGBs), as depicted as white and black lines, respectively.

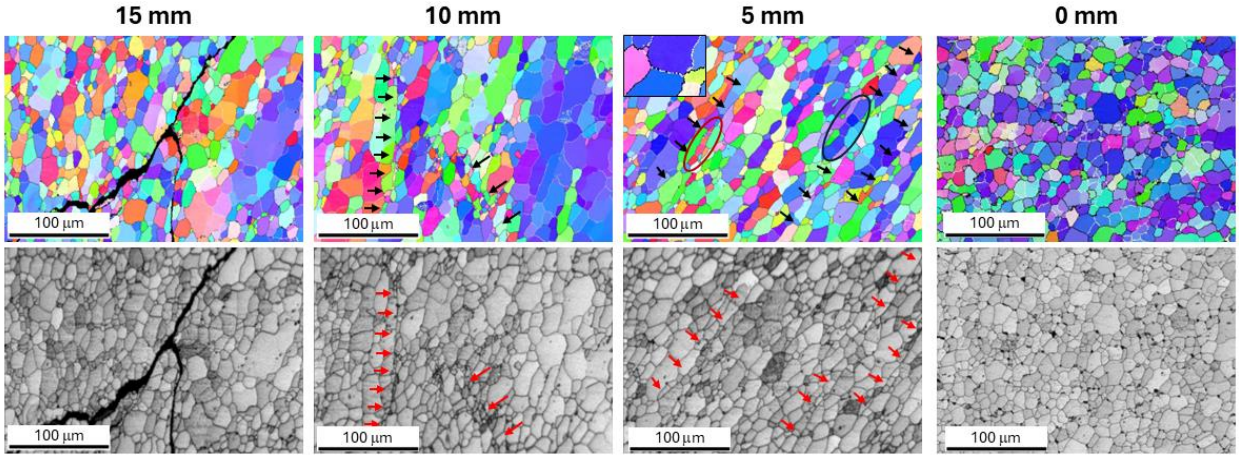

Figure 4. EBSD maps and SEM grain boundary contrast images were obtained at 15, 10, 5, and 0 mm positions. The arrows in the maps show chips boundaries, while highlighted ellipse show elongated grains because of high strain resulting from friction and compression.

The grain size distributions at distances of 15, 10, 5, and 0 mm demonstrate a clear location-dependent microstructural refinement. At 15 and 10 mm, the grain size histograms (Fig. 5) are broad and irregular, indicating chip-to-chip variability and heterogeneous deformation, with several larger grains contributing to higher mean diameters (~26.5 and 40.3 µm, respectively). In contrast, the distributions at 5 and 0 mm shift toward smaller sizes and become narrower, with lower mean grain sizes (~17.6 and 16.6 µm), showing a consistent reduction in average grain diameter. This overall decrease in grain size toward the position 0 mm indicates increasing microstructural refinement with decreasing distance.

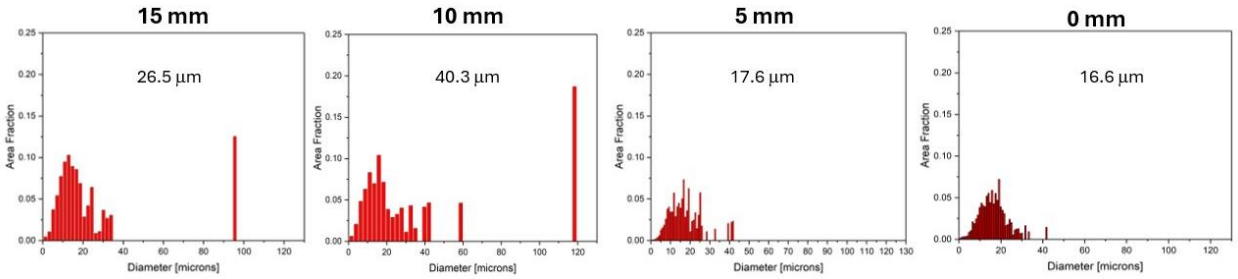

Figure 5. Grain size distributions and mean grain diameter at distances of 15, 10, 5, and 0 mm.

As the distance decreases towards the die-feedstock interface, the microstructure evolves from inhomogeneous chips to a homogeneous microstructure with fine equiaxed grains. The region at 15 mm consists of chips of varying sizes and exhibits an inhomogeneous grain structure. At 10 mm, there is no significant change in the microstructure other than the voids between the chips being closed as mentioned earlier. Nevertheless, it is still possible to observe the chip boundaries, as highlighted by the black and red arrows in the images. At the 5 mm region, the chips and grain structure are reoriented due to the geometrical strain imposed by the die rotation. Some LAGB segments transform into HAGBs due to progressive dislocation accumulation. Some elongated grains become thinner, and LAGBs form within the grains, subdividing the elongated grains into smaller subgrains.

Along with these elongated grains, misorientation angle measurements are presented in Fig. 6. An increase in the misorientation angle in Fig. 5a indicates that grain orientations evolve continuously due to subgrain rotation until exceeding 15° or transforming into HAGBs. The LAGB-to-HAGB transformation and subgrain rotation result in the formation of new grains, which is characteristic of the continuous dynamic recrystallization (CDRX) mechanism. In contrast, the subgrains inside elongated grains in Fig. 5b have similar grain orientation. With increasing strain, the elongated grains are geometrically pinched off into fine grains, indicating geometric dynamic recrystallization (GDRX) [3]. Further, as the material approaches the die interface (0 mm), plastic deformation leads to a gradual increase in boundary misorientation, refined grains, and promotes the transformation of LAGBs into HAGBs, resulting again in CDRX [18, 19].

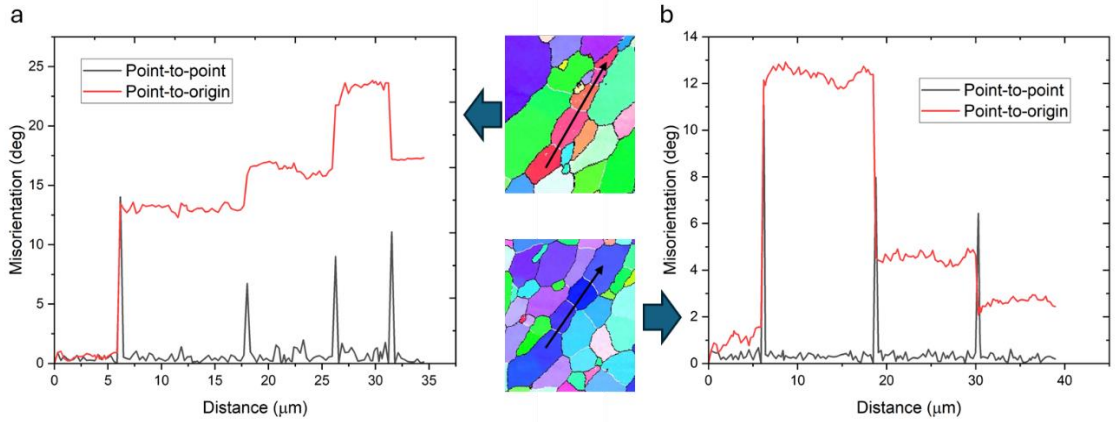

Figure 6. Misorientation along the arrows in the EBSD maps, indicated by (a) red ellipse and (b) black ellipse in region 5 mm in Fig. 4.

Supplement to that, the grain boundary misorientation results (shown in Fig. 7) at 15, 10, 5, and 0 mm do not follow a strict monotonic variation in the fractions of LAGBs and HAGBs. Nevertheless, the regions at 5 and 0 mm, which exhibit finer mean grain sizes, show a comparatively higher proportion of HAGBs, whereas the 15 and 10 mm locations contain relatively more LAGBs. This behavior is consistent with enhanced recrystallization and boundary transformation accompanying grain refinement during deformation.

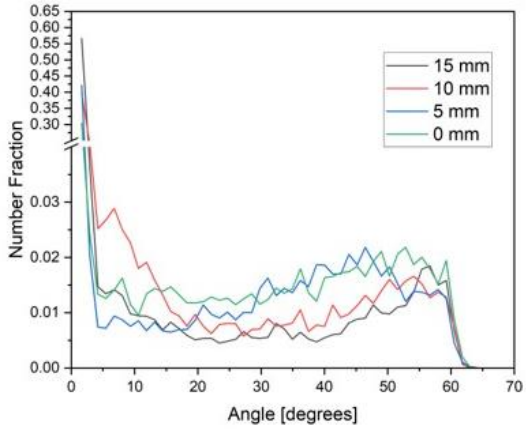

Figure 7. Grain boundaries misorientation angles distribution at distances of 15, 10, 5, and 0 mm, showing the relative fractions of LAGBs and HAGBs

c. Mechanism of chip bonding

To summarize the mechanism of chip bonding, Fig. 8, provides an overview of how bonding formation progresses through the different stages during FC. Initially, the voids exist among the compacted chips, the intermetallic particles are large, and the microstructure is inhomogeneous. Next, the microstructure and intermetallic particle size remain the same; however, the voids are partially closed, indicating compression. Afterwards, chip boundaries are consolidated, and mostly intermetallic particles in the matrix are broken into smaller particles and dispersed in the matrix, induced by severe plastic deformation as well as elevated temperatures. In the region close to the die, the material experiences even more severe plastic deformation and is exposed to high temperatures, leading to most particles being broken into smaller particles, the disappearance of chip boundaries, and grain refinement due to CDRX/GDRX, resulting in a homogeneous microstructure.

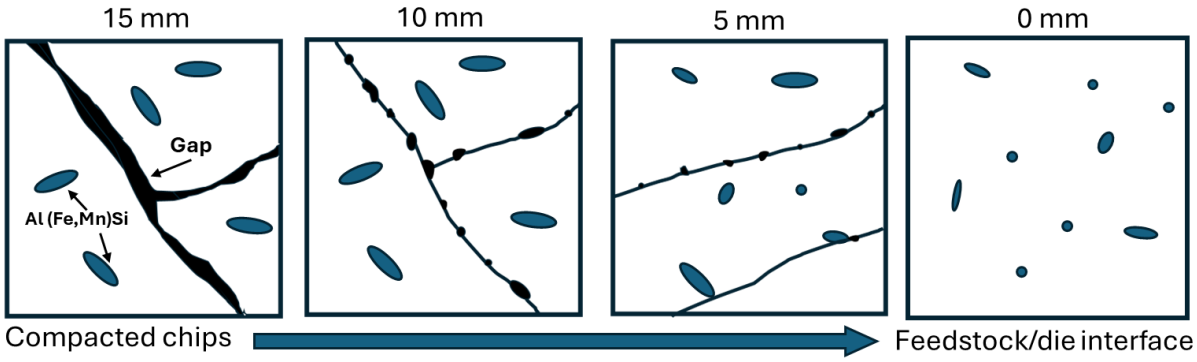

Figure 8. Progressive compression and bonding of irregular chips during the FE/FC process, evolving from weak initial interfacial contacts to full consolidation near the die interface.

4. Conclusion

This study shows that the residue of the compacted AA6082 chips formed during friction extrusion/consolidation in front of the die exhibits a pronounced gradient in bonding quality and microstructural development from the compacted chips base material towards the die interface. SEM and EBSD analyses reveal that, near the base material, the microstructure is inhomogeneous and contains a high density of LAGBs. As the material approaches the die interface, increasing strain promotes progressive subgrain rotation, leading to a gradual increase in boundary misorientation and the transformation of LAGBs into HAGBs causing CDRX. The chip boundaries contain voids near the base material, however, their presence is significantly reduced towards the die interface. Additionally, intermetallic particles are broken apart and dispersed within the matrix as a result of severe plastic deformation near the die interface. Overall, bonding quality changes noticeably within the residual compacted chips and becomes stronger from the base material toward the die. Consistent with this gradient, the measured grain size decreases toward the die interface, together with a relatively higher fraction of HAGBs in the refined regions, supporting progressive recrystallization and microstructural homogenization under increasing deformation.

5. Acknowledgement

This work was supported by German Research Foundation (DFG) within Priority Program SPP 2489 DaMic – subproject P8, *project number* 562138004.

6. References

[1] D. Raabe, D. Ponge, P.J. Uggowitzer, M. Roscher, M. Paolantonio, C. Liu, H. Antrekowitsch, E. Kozeschnik, D. Seidmann, B. Gault, F. De Geuser, A. Deschamps, C. Hutchinson, C. Liu, Z. Li, P. Prangnell, J. Robson, P. Shanthraj, S. Vakili, C. Sinclair, L. Bourgeois, and S. Pogatscher, Making sustainable aluminum by recycling scrap: The science of "dirty" alloys. Progress in Materials Science, 2022. 128: p. 100947.

[2] J. Gronostajski, J. Kaczmar, H. Marciniak, and A. Matuszak, Direct recycling of aluminium chips into extruded products. Journal of materials processing technology, 1997. 64(1-3): p. 149-156.

[3] U.F. Suhuddin, L. Rath, R.M. Halak, and B. Klusemann, Microstructure evolution and texture development during production of homogeneous fine-grained aluminum wire by friction extrusion. Materials Characterization, 2023. 205: p. 113252.

[4] D. Baffari, A.P. Reynolds, A. Masnata, L. Fratini, and G. Ingarao, Friction stir extrusion to recycle aluminum alloys scraps: Energy efficiency characterization. Journal of Manufacturing Processes, 2019. 43: p. 63-69.

[5] D. Baffari, G. Buffa, G. Ingarao, A. Masnata, and L. Fratini, Aluminium sheet metal scrap recycling through friction consolidation. Procedia Manufacturing, 2019. 29: p. 560-566.

[6] J. Lv, J. Yu, Z. Shi, W. Li, and J. Lin, Feasibility study of a novel multi-container extrusion method for manufacturing wide aluminium profiles with low force. Journal of Manufacturing Processes, 2023. 85: p. 584-593.

[7] R.M. Halak, L. Rath, U.F. Suhuddin, J.F. dos Santos, and B. Klusemann, Changes in processing characteristics and microstructural evolution during friction extrusion of aluminum. International Journal of Material Forming, 2022. 15(3): p. 24.

[8] W. Tang and A.P. Reynolds, Production of wire via friction extrusion of aluminum alloy machining chips. Journal of Materials Processing Technology, 2010. 210(15): p. 2231-2237.

[9] P. Noga, A. Piotrowicz, T. Skrzekut, A. Zwoliński, and P. Strzępek, Effect of various forms of aluminum 6082 on the mechanical properties, microstructure and surface modification of the profile after extrusion process. Materials, 2021. 14(17): p. 5066.

[10] W. Tang and A.P. Reynolds, Friction consolidation of aluminum chips. Friction Stir Welding and Processing VI, 2011: p. 289-298.

[11] G.Poy Ignacio, L. Rath, U.F. Suhuddin, and B. Klusemann, Friction extrusion from AlMgSi machining waste at high extrusion ratio. Materials Research Proceedings. 54.

[12] M.K. Mejbel, S.K. Hussein, and I.T. Abdullah, Friction stir consolidation for recycling AA6061 chips with its metal flow investigation for billet production. Journal of Engineering Research, 2025. 13(2): p. 1170-1183.

[13] R. Puleo, A. Latif, G. Ingarao, R. Di Lorenzo, and L. Fratini, Solid bonding criteria design for aluminum chips recycling through Friction Stir Consolidation. Journal of Materials Processing Technology, 2023. 319: p. 118080.

[14] R. Puleo, A. Latif, G. Ingarao, and L. Fratini, A generalized parametric model for the bonding occurrence prediction in friction stir consolidation of aluminum alloys chips. Journal of Manufacturing Processes, 2024. 131: p. 604-618.

[15] L. Rath, U.F. Suhuddin, and B. Klusemann, Comparison of friction extrusion processing from bulk and chips of aluminum-copper alloys. Key Engineering Materials, 2022. 926: p. 471-480.

[16] C. Liu, Q. Du, N. Parson, and W.J. Poole, The interaction between Mn and Fe on the precipitation of Mn/Fe dispersoids in Al-Mg-Si-Mn-Fe alloys. Scripta Materialia, 2018. 152: p. 59-63.

[17] M.N. Rahaman, Ceramic processing and sintering. 2017: CRC press.

[18] S. Gourdet and F. Montheillet, A model of continuous dynamic recrystallization. Acta Materialia, 2003. 51(9): p. 2685-2699.

[19] H. McQueen, Development of dynamic recrystallization theory. Materials Science and Engineering: A, 2004. 387: p. 203-208.